1 Introduction

Energy is one of the strongest contributors to economic growth. In the future, economies will continue to grow, populations will do so too, and their energy demand will accompany such growth [7] [12]. Meeting these future needs requires the development of clean energy sources as environmental concerns continue to rise.

As seen in Figure 1, electricity generation was one of the economic sectors that released the most greenhouse gases (GHGs) in the United States (US) in 2017. As carbon dioxide (CO_2) is the main component in GHGs, decarbonizing electricity generation will allow us to meet the increases in energy demand and address the environmental concerns at the same time.
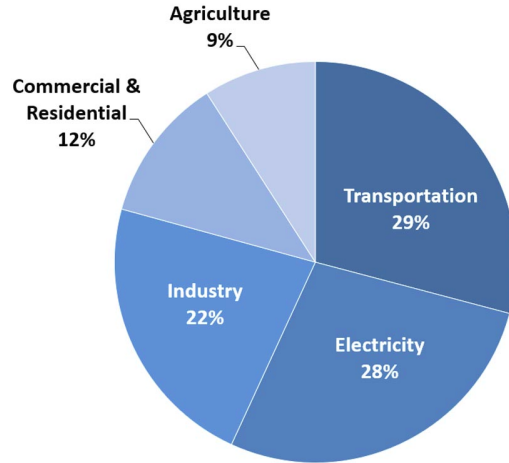

Figure 1: Total US GHG emissions by economic sector in 2017. Image reproduced from [14].

To address these concerns, utility companies are relying more and more on renewable energy resources, such as wind and solar [20]. However, high solar adoption creates a challenge. The need for electricity generators to quickly ramp up increases when the sun sets and the contribution from the photovoltaics (PV) falls [23]. The "duck curve" (or duct chart) depicts this phenomenon, Figure 2. The California ISO (CAISO) developed the duck curve to illustrate the net load of the grid [5]. We define the net load as the difference between forecasted load and expected electricity production from solar.

Moreover, the duck curve reveals another issue. Over-generation may occur during the middle of the day and high-levels of non-dispatchable generation may exacerbate the situation. As a consequence, the market would experience sustained zero or negative prices during the middle of the operating day [5].

The simplest solution to a demand ramp up is to increase dispatchable generation, resources with fast ramping and fast starting capabilities such as natural gas and coal [5], and, consequently, decrease non-dispatchable generation, such as geothermal, nuclear, and hydro. Nonetheless, an approach like this is not consistent with the goal of reducing carbon emissions. Hence, our focus drifts to other potential low-carbon solutions, like nuclear generation and electricity storage by means of hydrogen (H_2) production.

Unfortunately, a carbon neutral electric grid will be insufficient to halt climate change because transportation is a big contributor to GHG emissions. As seen in Figure 1, transportation released the most GHGs in the US in 2017. Thus, decarbonizing transportation underpins global carbon reduction.

One possible strategy is to develop a hydrogen economy, as Japan is currently doing. Japan's strategy rests on the firm belief that H_2 can be a decisive response to its energy and climate challenges.
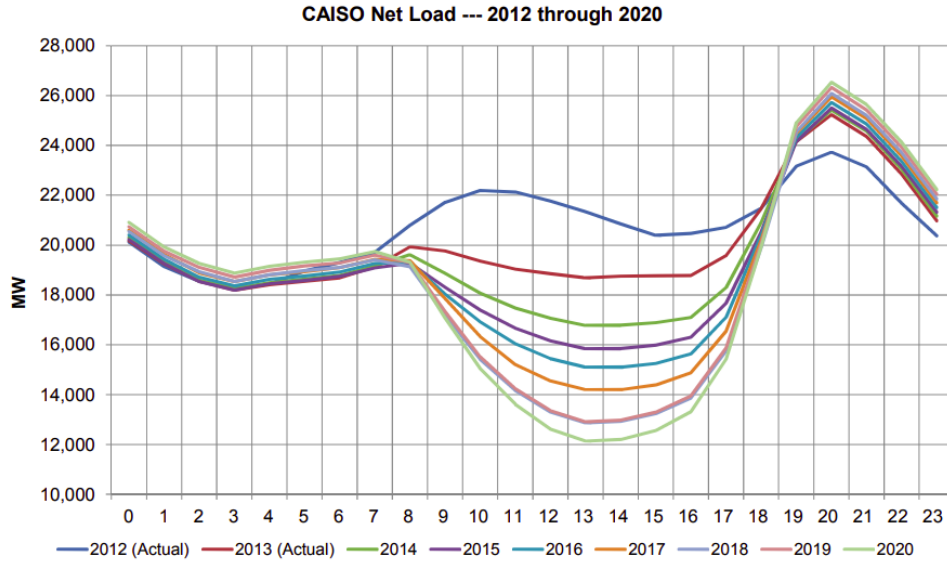
Figure 2: The duck curve. Image reproduced from [5].

It could foster deep decarbonization of the transport, power, industry, and residential sectors while strengthening energy security [21]. In the transportation sector, Japan is planning to deploy fuel cell vehicles, trucks, buses, trains, and ships.

Although H_2 technologies do not release CO_2, any H_2 production method is only as carbon-free as the source of energy it relies on (electric, heat, or both). Nuclear reactors present a clean energy option to manufacture H_2.

The University of Illinois at Urbana-Champaign (UIUC) is leading by example and actively working to reduce GHG emissions from electricity generation and transportation (among other sectors) on its campus. In pursuance of those efforts, the university has developed the Illinois Climate Action Plan (iCAP).

2   iCAP

In 2008, UIUC signed the American College and University Presidents' Climate Commitment, formally committing to become carbon neutral as soon as possible, no later than 2050. The university developed the first iCAP in 2010 as a comprehensive roadmap toward a sustainable campus environment [25]. The iCAP defines a list of goals, objectives, and potential strategies for the following six topical areas.

- Energy Conservation and Building Standards:

Focuses on maintaining or reducing campus gross square footage, strengthen conservation efforts, and engage the campus community in energy conservation.

- Energy Generation, Purchasing, and Distribution:

Efforts towards the exploration of 100% clean campus energy options. This includes the expansion of on-campus solar energy production, the expansion of the purchase of clean energy from low-carbon energy sources, and the offset of all emissions from the National Petascale Computing Facility.

- Transportation:

2

This area comprises the efforts on reducing air travel emissions, reducing Urbana-Champaign campus fleet emissions, and also studying scenarios for complete conversion of the campus fleet to renewable fuels.

- Water and Stormwater:

This area focuses on improving water efficiency of cooling towers, perform a water audit to establish water conservation targets, determine upper limits for water demand by end-use, and implement projects to showcase the potential of water and stormwater reuse.

- Purchasing, Waste, and Recycling:

Attempt to standardize the purchases of office paper, cleaning products, computers, other electronics, and freight delivery services. It also attempts to foment recycling by reducing non-durable goods purchases and reducing municipal solid waste going to landfills.

- Agriculture, Land Use, Food, and Sequestration:

This area will perform a comprehensive assessment of GHG emissions from agricultural operations, and develop a plan to reduce them, implement a project that examines the food service carbon footprint for Dining, and increase carbon sequestration in campus soils.

3   Objectives

As mentioned earlier, we place our attention on two areas: electricity generation and transportation. We will turn our attention to the electricity generation and transportation in the UIUC campus. Consequently, the objective of this work aligns with the efforts in two of the six target areas defined on the iCAP.

Regarding electricity generation, our analysis focuses on the UIUC grid. The present work quantifies the magnitude of the duck curve in such grid. To mitigate the risk of over-generation, we propose to use the over-generated energy to manufacture H_2. We chose a nuclear reactor to be the main source of energy. The next step is to quantify how much H_2 different production methods are able to produce. Section 4 discusses a few hydrogen production methods considered for our analysis. Finally, we will calculate how much electricity we would generate using the H_2 produced.

Regarding transportation, we study the conversion of the UIUC fleet on campus to Fuel Cell Electric Vehicles (FCEVs). Additionally, the analysis includes the conversion of the Champaign-Urbana Mass Transit District (MTD) fleet as well. The first step is to determine the fuel consumed by both fleets and how much H_2 enables the complete conversion of the fleets. Finally, we consider a few reactor designs and analyze which of them could produce enough H_2 to fulfill both fleet requirements.

Both studies propose the same solution, a nuclear reactor coupled to a hydrogen plant. In terms of electricity generation, this solution will decrease the need for dispatchable sources and, consequently, reduce the carbon emissions. In terms of transportation, it will eliminate carbon emissions.

In both analyses, many reactor choices can satisfy our needs. The typical UIUC's grid demand is smaller than 80 MW [11]. Accordingly, we consider reactors of small capacities, such as microreactors and Small Modular Reactors (SMRs). Section 5 discusses their characteristics.

4   Hydrogen production methods

This section introduces several hydrogen production processes and their energy requirements.

4.1 Electrolysis

The electrolysis of water is a well-known method whose commercial use began in 1890. This process produces approximately a 4% of H_2 worldwide. The process is ecologically clean because it does not emit GHGs. However, in comparison with other methods, electrolysis is a highly energy-demanding technology [19].

Three electrolysis technologies exist. Alkaline-based is the most common, the most developed, and the lowest in capital cost. It has the lowest efficiency and, therefore, the highest electrical energy cost. Proton exchange membrane electrolyzers are more efficient but more expensive than Alkaline electrolyzers. Solide Oxide Electrolysis Cells (SOEC) electrolyzers are the most electrically efficient but the least developed. SOEC technology has challenges with corrosion, seals, thermal cycling, and chrome migration [19]. As the first two technologies work with liquid water and the latter requires high temperature steam, we will refer to the first two as Low Temperature Electrolysis (LTE) and the latter as High Temperature Electrolysis (HTE).

Water electrolysis converts electric and thermal energy into chemical energy stored in hydrogen. The process enthalpy change ΔH determines the required energy for the electrolysis reaction to take place. Part of the energy corresponds to electric energy ΔG and the rest of it to thermal energy $T \cdot \Delta S$, Equation 1.

$$\Delta H = \Delta G + T\Delta S \tag{1}$$

where

$$\Delta H = \text{Total specific energy [kWh/kg-H}_2\text{]} \tag{2}$$
$$\Delta G = \text{Specific electrical energy [kWh/kg-H}_2\text{]} \tag{3}$$
$$T\Delta S = \text{Specific thermal energy [kWh/kg-H}_2\text{]}. \tag{4}$$

In LTE, electricity generates the thermal energy. Hence, ΔH alone determines the process required energy. ΔH is equal to 60 kWh/kg-H_2 considering a 67% efficiency [29].

In HTE, a high temperature heat source is necessary to provide the thermal energy. ΔG decreases with increasing temperature, Figure 3. Decreasing the electricity requirement results in higher overall production efficiencies since heat-engine-based electrical work has a thermal efficiency of 50% or less [18]. Figure 3 shows ΔG and $T\Delta S$. ΔG considers the SOEC to have an electrical efficiency of an 88% [16]. $T\Delta S$ accounts for the latent heat of water vaporization. Note that the process is at 3.5 MPa. ΔG increases with pressure. However, we chose a high pressure to save energy, as compressing liquid water is cheaper than compressing the hydrogen [26].

Finally, equations 5 and 6 determine the electrical P_{EH2} and thermal power P_{TH2} required by the hydrogen plant.

$$P_{EH2} = \dot{m}_{H2}\Delta G \tag{5}$$
$$P_{TH2} = \dot{m}_{H2}T\Delta S \tag{6}$$

where

$$P_{EH2} = \text{Total electrical power [kW]} \tag{7}$$
$$P_{TH2} = \text{Total thermal power [kW]} \tag{8}$$
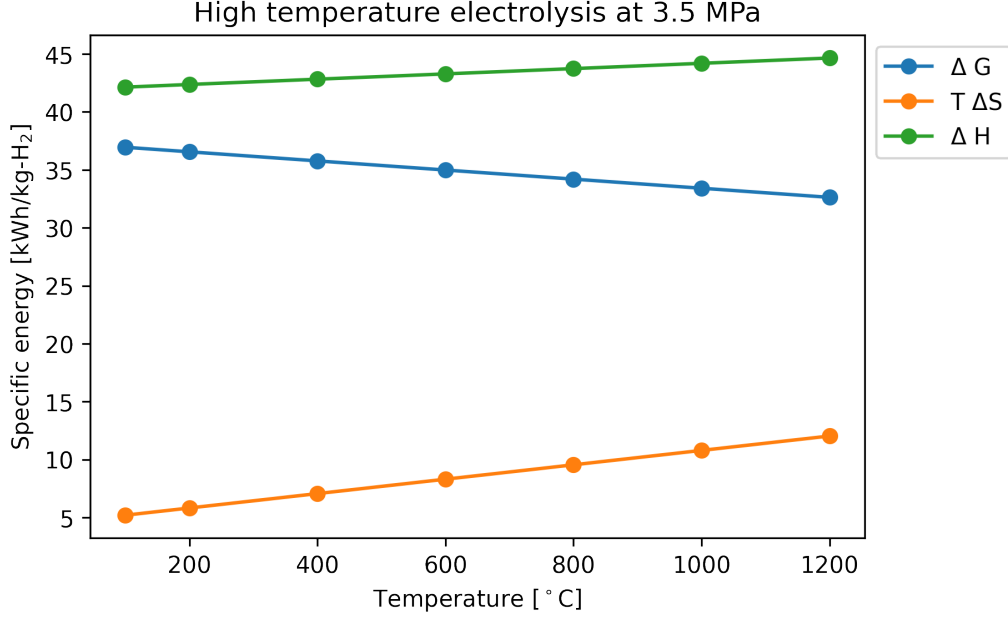$$\dot{m}_{H2} = \text{H}_2 \text{ production rate [kg/h]}. \tag{9}$$

Figure 3: Energy required by HTE at 3.5 MPa.

4.2 Sulfur-Iodine Thermochemical Cycle

Thermochemical water-splitting is the conversion of water into hydrogen and oxygen by a series of thermally driven chemical reactions. The direct thermolysis of water requires temperatures above 2500 °C for significant hydrogen generation. At this temperature, the process can decompose a 10% of the water. A thermochemical water-splitting cycle accomplishes the same overall result using much lower temperatures.

General Atomics, Sandia National Laboratories, and the University of Kentucky compared 115 cycles that would use high temperature heat from an advanced nuclear reactor [6]. The report specifies a set of screening criteria used to rate each cycle. The highest scoring method was the Sulfur-Iodine (SI) Cycle.

The SI cycle consists of the three chemical reactions represented in Figure 4. The whole process takes in water and high temperature heat, and releases hydrogen and oxygen. The process does not use any electricity. The process recycles all reagents and does not have any effluents [32]. The chemical reactions are:
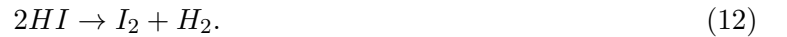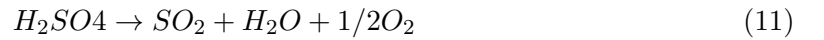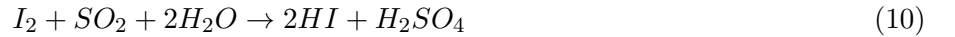
$$I_2 + SO_2 + 2H_2O \rightarrow 2HI + H_2SO_4 \tag{10}$$
$$H_2SO4 \rightarrow SO_2 + H_2O + 1/2O_2 \tag{11}$$
$$2HI \rightarrow I_2 + H_2. \tag{12}$$

Figure 5 presents the specific energy requirements of the cycle ΔH. Several sources disagree on the minimum temperature for the process to be viable. Our analysis considers the process viable only for temperatures above 800 °C. Finally, equation 13 determines the thermal power P_{TH2} required by the hydrogen plant.

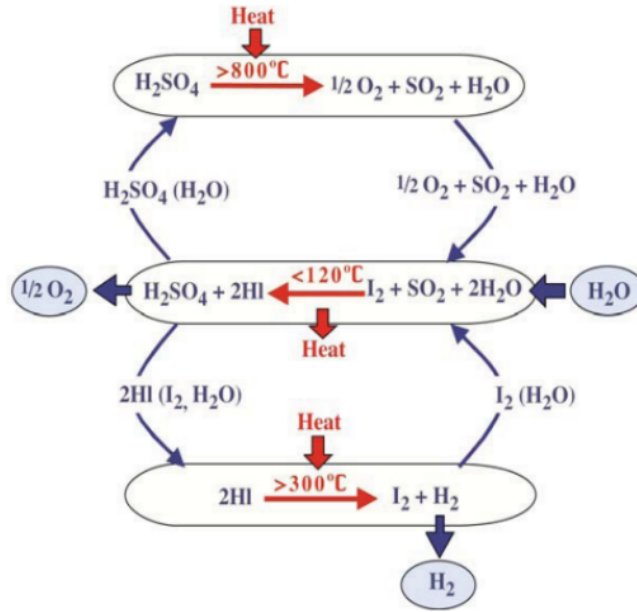$$P_{TH2} = \dot{m}_{H2}\Delta H \tag{13}$$

5

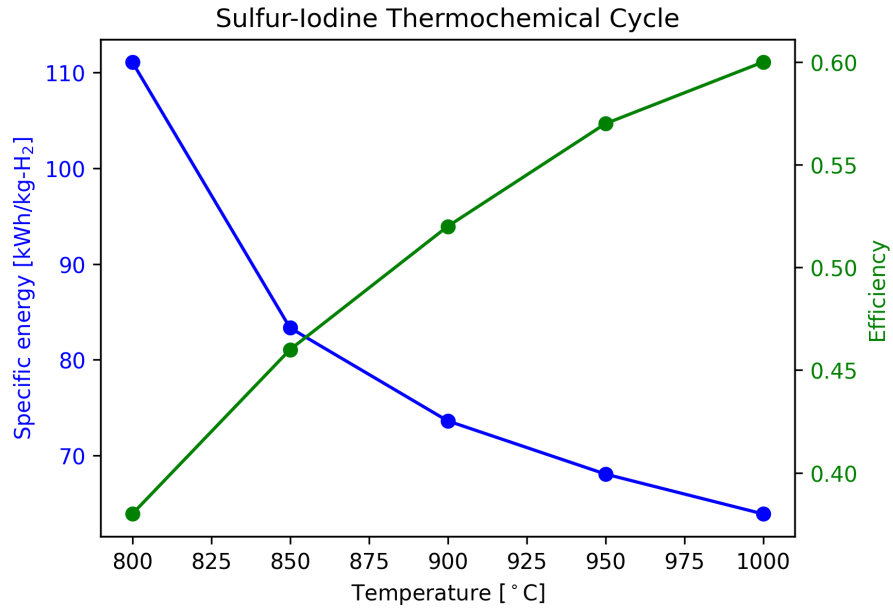Figure 4: Diagram of the Sulfur-Iodine Thermochemical process. Image reproduced from [4].

Figure 5: Energy required by the Sulfur-Iodine Thermochemical Cycle.

where

$$P_{TH2} = \text{Total thermal power [kW]} \tag{14}$$
$$\dot{m}_{H2} = \text{H}_2 \text{ production rate [kg/h]} \tag{15}$$
$$\Delta H = \text{Specific energy [kWh/kg-H}_2\text{]}. \tag{16}$$

5 Microreactors and SMRs

These reactor concepts share several features. The reactors require limited on-site preparation as their components are factory fabricated and shipped out to the generation site. This feature reduces up-front capital costs, enables rapid deployment, and expedites start-up times. This reactor concept allows for black starts and islanding operation mode. They can start up from a completely de-energized state without receiving power from the grid. They can also operate connected to the grid or independently. Moreover, these type of reactors are self-regulating. They minimize electrical parts and use passive safety systems to prevent overheating and safely shutdown.

Microreactors have the distinction that are transportable. Small designs make it easy for vendors to ship the entire reactor by truck, shipping vessel, or railcar. These features make the technology appealing for a wide range of applications, such as deployment in remote residential locations and military bases.

The Department of Energy (DOE) defines a microreactor as a reactor that generates from 1 to 20 MW$_{th}$ [28]. The International Atomic Energy Agency (IAEA) describes a SMR as a reactor whose power is under 300 MWe. It defines, as well, a very small modular reactor as a reactor that produces less than 15 MWe [3]. As the definitions of these reactor concepts overlap, we will consider reactors of less than 100 MW$_{th}$ regardless of their specific classification.

6 Methodology

In this analysis, the energy source (both electric and thermal) is a nuclear reactor with co-generation capabilities. The nuclear reactor supplies the grid with electricity P_E while providing a hydrogen plant with electricity P_{EH2} and thermal energy P_{TH2}, see the diagram in Figure 6. β and γ determine the distribution of the reactor thermal power P_{th} into P_E, P_{EH2}, and P_{TH2}, see Equations 17 to 22.
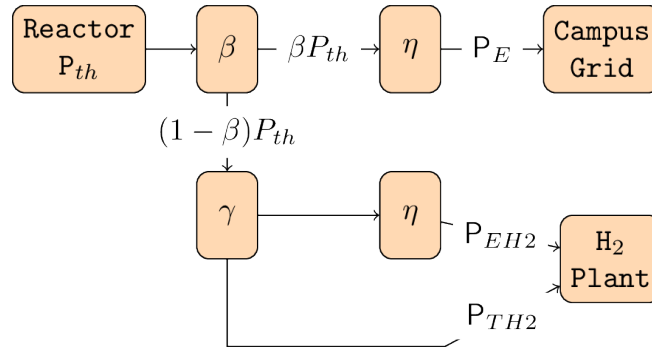

Figure 6: Diagram of a reactor coupled to hydrogen plant.

$$P_E = \eta \beta P_{th} \tag{17}$$
$$P_{EH2} = \eta \gamma (1 - \beta) P_{th} \tag{18}$$
$$P_{TH2} = (1 - \gamma)(1 - \beta) P_{th} \tag{19}$$

where

$$\eta = \text{thermal-to-electric conversion efficiency} \tag{20}$$

$$\beta = \frac{P_E/\eta}{P_E/\eta + P_{TH2}/(1-\gamma)} \tag{21}$$

$$\gamma = \frac{P_{EH2}/\eta}{P_{EH2}/\eta + P_{TH2}}. \tag{22}$$

If $\beta = 1$, the reactor only supplies the grid with electricity P_E and the hydrogen plant does not produce H_2. If $\beta = 0$, the reactor only supplies the hydrogen plant and no electricity goes into the grid. Table 1 summarizes the values that γ takes for the different methods.

| Method	γ	P_{EH2}	P_{TH2}
LTE	1	$\neq 0$	0
HTE	$0 < \gamma < 1$	$\neq 0$	$\neq 0$
SI	0	0	$\neq 0$

Table 1: Energy requirements of the different methods.

7 Results

This section holds the results of the different analyses.

7.1 Transportation

This subsection centers its focus on the transportation sector. Figure 7 displays the fuel consumed per day by MTD and UIUC fleet. Using the values shown in Table 2, we calculate the H_2 requirement for MTD and UIUC fleets, Figure 8. Table 3 summarizes the most important results.
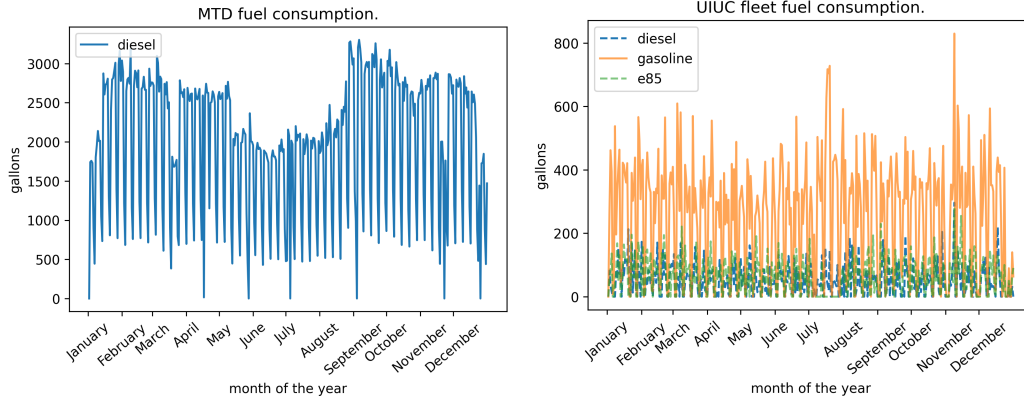
(a) MTD fleet. Data go from July 1, 2018, until June 30, 2019 [10].

(b) UIUC fleet. Data go from January 1, 2019, until December 31, 2019 [31].

Figure 7: Fuel consumption.

Using Table 4, we calculate the CO_2 savings caused by replacing all the fossil fuels by H_2. Table 5 displays the CO_2 savings for both fleets.

Table 2: H_2 necessary to replace a gallon of fuel [24] [8].

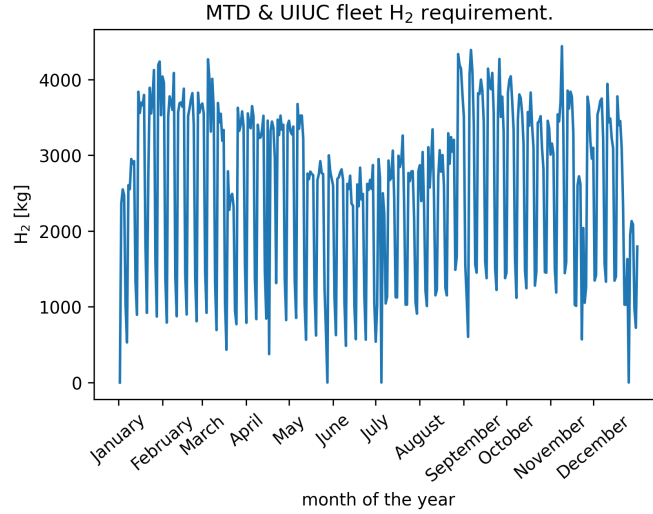|	Hydrogen Mass [kg]
Gasoline	1
Diesel	1.13
E85	0.78

Figure 8: H_2 requirement for MTD and UIUC fleets.

Table 3: H_2 requirement for MTD and UIUC fleets.

Total [tonnes/year]	943
Average [kg/day]	2584
Average [kg/h]	108
Maximum in one day [kg]	4440

Table 4: CO_2 savings in lbs per gallon of fuel burned [1].

	CO_2 produced [lbs/gallon]
Gasoline	19.64
Diesel	22.38
E85	13.76

Table 5: CO_2 yearly savings.

	CO_2 mass [tonnes/year]
MTD	7306
UIUC	1143
Total	8449

We have determined the H$_2$ requirement by the fleets, now we seek for a microreactor design that is capable of meeting such demand. For our analysis we chose a few microreactor designs summarized in Table 6. Further studies could include other designs as well.

Figure 9 shows the hourly production rates for the different reactors and the different H$_2$ production processes. The figure includes a continuous line that represents the hydrogen requirement of both fleets. Note that the high temperatures required by the SI process allow for the coupling with only one microreactor design which has an outlet temperature of more than 800[°]C.

Table 6: Microreactor designs.

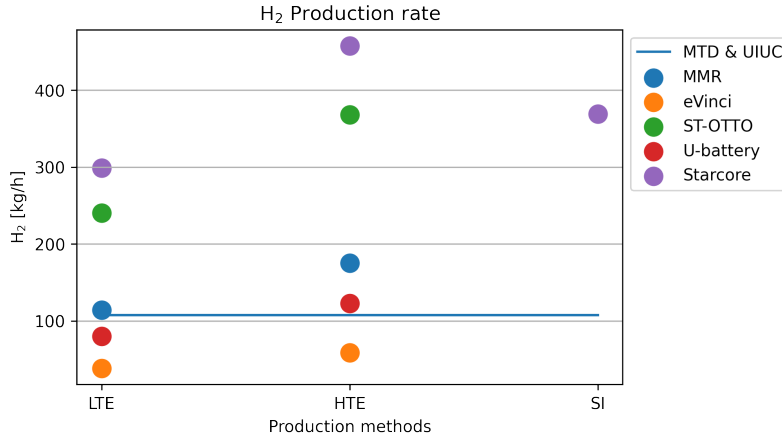| Reactor	P[MW$_{th}$]	T$_o$[°C]
MMR [30]	15	640
eVinci [17]	5	650
ST-OTTO [15]	30	750
U-battery [9]	10	750
Starcore [22]	36	850

Figure 9: Hydrogen production rate by the different microreactor designs.

7.2 Electricity Generation

This subsection centers its focus on the electricity generation sector and the duck curve problem. In order to quantify the magnitude of the duck curve, we have to predict the load of the UIUC grid and the expected electricity production from solar. As the iCAP main objective is to become carbon neutral before 2050, we do our prediction for that year. UIUC solar farm is relatively new, and the data available is not enough for producing a reliable prediction. To go around this barrier, we use the available data for the whole US. Figure 10 displays the prediction for 2050. We carry out the prediction by means of a linear regression that produces the worst scenario. In such scenario the total load does not increase considerably whereas the solar generation does.

The next step was to apply the same growth factor from the predictions to the load of the UIUC grid and the solar electricity. We apply the growth factor to the hourly data of a day in the spring of 2019 to obtain a prediction for 2050. We choose the spring when the solar production is higher, as it is sunny, but the total load is low since people are not using electricity for air conditioning or heating [23]. Finally, we substract the solar production from the total load, obtaining the net load or demand (D_{NET}). We narrowed the focus of our analysis to April 4th, when the net demand reached the lowest

(a) Total electricity generation.
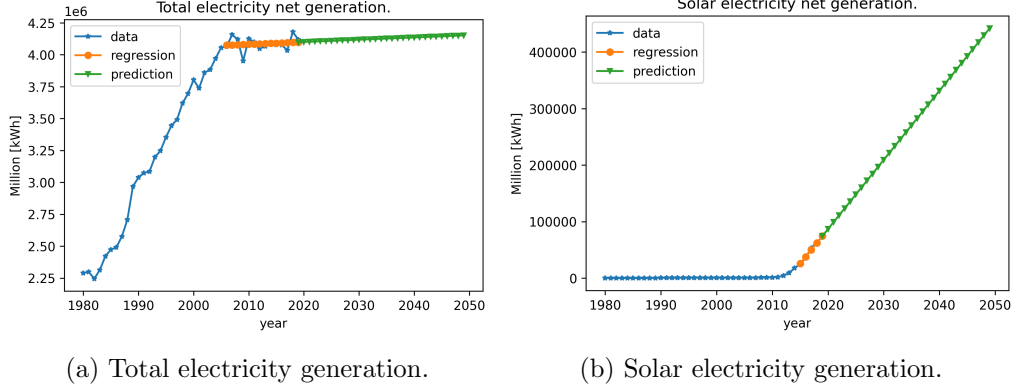
(b) Solar electricity generation.

Figure 10: Prediction of the electricity generation in the US for 2050. Data from [2].

value in the spring. Figure fig:uiuc-duck1 shows these results. In 2050, the peak net demand will be 46.9 MWh at 5 PM. The lowest net demand will be 15 MWh at 11 AM. This yields a demand ramp of 31.9 MWh in 4 hours. These results show that the grid requires an available capacity of dispatchable sources of at least 31.9 MW.
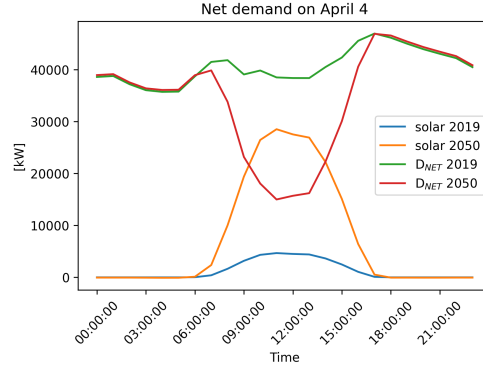

Figure 11: Prediction of UIUC's net demand for 2050.

Once we calculated the net demand, the next step was to calculate the over-generated electricty. For that, we arbitrarily chose a reactor of 25 MW. For the LTE case, any type of reactor is a valid option. We chose an η of 33% This yields a reactor power of 75.8 MW$_{th}$.

For the HTE case, the choice of a reactor is a High Temperature Gas-Cooled Reactor (HTGR) with an outlet temperature of 850°C. We consider an η of 49.8%. This yields a reactor of 50.2 MW$_{th}$.

We consider that the reactor operates at full capacity at all times. However, the reactor electricity (P_E) equals the net demand (D_{NET}) once it is smaller than 25 MW. Note that P_E has power units while D_{NET} has energy units. We chose time steps of 1 hour for our analysis, hence P_E and D_{NET} differ by the constant h. As P_E is lower than 25 MW, and the reactor is at full thermal capacity, the excess of thermal energy is directed to the hydrogen plant. We use equation 23 with equations 17 to 22 to calculate the hydrogen produced. Figure 12 displays the results. The total H$_2$ production reaches 660, 1009, and 815 kg for LTE, HTE, and SI, respectively.

$$P_E = D_{NET}$$
$$\frac{P_E}{25MW} = \frac{\eta\beta P_{th}}{\eta P_{th}} = \beta \tag{23}$$
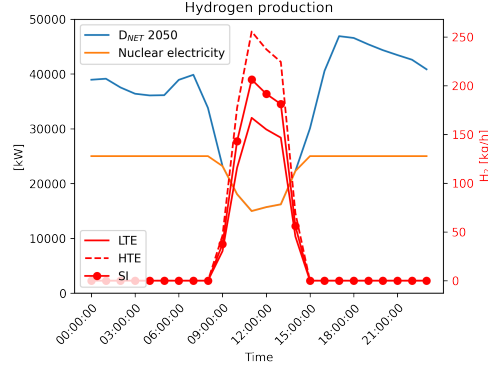
Figure 12: H_2 production.

The last step in our analysis is to calculate the reduction of the peak demand by using the hydrogen to produce electricity. The energy produced by hydrogen is $285 kJ/mol$, which is equal to 40 kWh/kg [27]. However, convetional fuel cells can use up to a 60% of that energy [13]. Knowing the mass of hydrogen produced, we calculate the total electricity produced. We know reduce the peak demand by distributing the electricity over a certain range of hours. We chose to distribute the electricity produced over the course of 6 hours. We calculate the new peak using equation 25. Figure 13 shows these results. The different H_2 processes are able to generate 15.84 MWh, 24.2 MWh, and 19.6 MWh, respectively. This accounts for a peak reduction of 5 MW, 6.4 MW, and 5.6 MW, respectively.

$$NP = \frac{\sum_{i=0}^{N} D_{NET,i} - TH}{N} \tag{24}$$

$$\tag{25}$$

where

$$NP = \text{New peak magnitude} \tag{26}$$
$$D_{NET,i} = \text{Hourly net demant} \tag{27}$$
$$TH = \text{Total mass oh hydrogen} \tag{28}$$
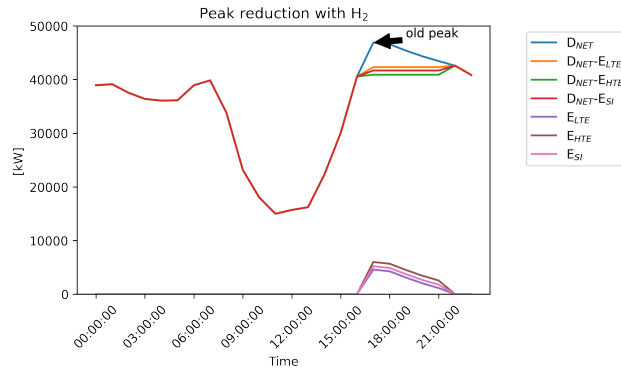$$N = \text{Total number of hours when we use the } H_2 \tag{29}$$

Figure 13: Peak reduction by using the produced H_2.

8   Conclusions

The University of Illinois is actively working to reduce GHG emissions on its campus.

A few microreactor designs could produce enough hydrogen to meet MTD and UIUC fleet fuel demand.

Increased solar penetration worsens the duck curve.

Hydrogen introduces a way to store energy that reduces the reliance on dispatchable sources.

Nuclear energy and hydrogen production present an approach to mitigate the negative implications of the duck curve.

References

[1] Energy Information Administration. How much carbon dioxide is produced by burning gasoline and diesel fuel?, April 2014.

[2] US Energy Information Administration. Electric Power Monthly with data for February 2020. page 273, April 2020.

[3] World Nuclear Association. Small nuclear power reactors - World Nuclear Association, June 2020.

[4] Benjamin Russ. Sulfur Iodine Process Summary for the Hydrogen Technology Down-Selection. Technical Report INL/EXT-12-25773, 1047207, May 2009.

[5] Brad Bouillon. Prepared Statement of Brad Bouillon on behalf of the California Independent System Operator Corporation, June 2014.

[6] Lc Brown, Ge Besenbruch, Rd Lentsch, Kr Schultz, Jf Funk, Ps Pickard, Ac Marshall, and Sk Showalter. HIGH EFFICIENCY GENERATION OF HYDROGEN FUELS USING NUCLEAR POWER. Technical report, GENERAL ATOMICS (US), June 2003.

[7] Paul J. Burke, David I. Stern, and Stephan B. Bruns. The Impact of Electricity on Economic Development: A Macroeconomic Perspective. *International Review of Environmental and Resource Economics*, 12(1):85–127, November 2018.

[8] Alternative Fuels Data Center. Fuel Properties Comparison, October 2014.

[9] Ming Ding, J. L. Kloosterman, Theo Kooijman, and Rik Linssen. Design of a U-Battery. Technical Report PNR-131-2011-014, Urenco, and Koopman and Witteveen, November 2011.

[10] Champaign-Urbana Mass Transit District. Champaign-Urbana Mass Transit District Public Records, December 2019.

[11] Samuel G. Dotson and Kathryn D. Huff. Optimal Sizing of a Micro-Reactor for Embedded Grid Systems. In *Transactions of the American Nuclear Society Student Conference*, Raleigh, N.C., March 2020. American Nuclear Society.

[12] Mostafa El-Shafie, Shinji Kambara, and Yukio Hayakawa. Hydrogen Production Technologies Overview. *Journal of Power and Energy Engineering*, 07(01):107–154, 2019.

[13] DOE Energy Efficiency and Renewable Energy. Fuel cells fact sheet, November 2015.

[14] US EPA. Sources of Greenhouse Gas Emissions, January 2020.

[15] Bowers Harlan. X-energy Xe-100 Reactor initial NRC meeting, September 2018.

[16] HELMETH. High temperature electrolysis cell (SOEC), February 2020.

[17] Richard Hernandez, Michael Todosow, and Nicholas R. Brown. Micro heat pipe nuclear reactor concepts: Analysis of fuel cycle performance and environmental impacts. *Annals of Nuclear Energy*, 126:419–426, April 2019.

[18] J. E. O'Brien, C. M. Stoots, J. S. Herring, M. G. McKellar, E. A. Harvego, M. S. Sohal, and K. G. Condie. High Temperature Electrolysis for Hydrogen Production from Nuclear Energy TechnologySummary. Technical Report INL/EXT-09-16140, 978368, February 2010.

[19] Christos M. Kalamaras and Angelos M. Efstathiou. Hydrogen Production Technologies: Current State and Future Developments. *Conference Papers in Energy*, 2013:1–9, 2013.

[20] Zach Ming, Arne Olson, Huai Jiang, Manohar Mogadali, and Nick Schlag. Resource Adequacy in the Pacific Northwest, March 2019.

[21] Monica Nagashima and Institut français des relations internationales. *Japan's hydrogen strategy and its economic and geopolitical implications.* 2018. OCLC: 1059514336.

[22] Star Core Nuclear. Star Core Spec Sheet, December 2015.

[23] U.S. Department of Energy. Confronting the Duck Curve: How to Address Over-Generation of Solar Energy, October 2017.

[24] DOE Office of Energy Efficiency and Renewable Energy. Hydrogen Production Processes, 2020. Library Catalog: www.energy.gov.

[25] University of Illinois at Urbana-Champaign. Illinois Climate Action Plan, 2015.

[26] J E O'Brien, J S Herring, C M Stoots, M G McKellar, E A Harvego, K G Condie, G K Housley, and J J Hartvigsen. Status of the INL High- Temperature Electrolysis Research Program – Experimental and Modeling. page 13, April 2019.

[27] Alfredo Ursua, Luis M. Gandia, and Pablo Sanchis. Hydrogen Production From Water Electrolysis: Current Status and Future Trends. *Proceedings of the IEEE*, 100(2):410–426, February 2012.

[28] US-DOE. The Ultimate Fast Facts Guide to Nuclear Energy. Fact Sheet DOE/NE-0150, Department of Energy Office of Nuclear Energy, Washington D.C., January 2019. https://www.energy.gov/ne/downloads/ultimate-fast-facts-guide-nuclear-energy.

[29] USDRIVE. Hydrogen Production Tech Team Roadmap, November 2017.

[30] USNC. MMR - USNC, 2019.

[31] Pete Varney. Personal Communication, January 2020.

[32] B Yildiz and M Kazimi. Efficiency of hydrogen production systems using alternative nuclear energy technologies. *International Journal of Hydrogen Energy*, 31(1):77–92, January 2006.